Membrane-Type 4 Matrix Metalloproteinase (MT4-MMP) induces lung metastasis by alteration of primary breast tumor vascular architecture

Vincent CHABOTTAUX[1], Stéphanie RICAUD[2,3], Laurent HOST[1], Silvia BLACHER[1], Alexandra PAYE[1], Marc THIRY[4], Anikitos GAROFALAKIS[2,3], Carine PESTOURIE[2,3], Karine GOMBERT[2,3], Françoise BRUYERE[1], Daniel LEWANDOWSKY[5], Bertrand TAVITIAN[2,3], Jean-Michel FOIDART[1,6], Frédéric DUCONGE[2,3] and Agnès NOEL[1, *]

(1) Laboratory of Tumor and Developmental Biology, Groupe Interdisciplinaire de Génoprotéomique Appliquée-Cancer (GIGA-Cancer), University of Liege, Tour de Pathologie (B23), B-4000 Liège, Belgium ; (2) CEA, DSV, Institut d'Imagerie Biomédicale (I²BM), Service Hospitalier Frédéric Joliot, Laboratoire d'Imagerie Moléculaire Expérimentale, 4 place du général Leclerc, 91401 Orsay Cedex, France ; (3) INSERM U803, 4 place du général Leclerc, 91401 Orsay Cedex, France ; (4) Laboratory of Cell and Tissue Biology, University of Liège, B-4000 Liège, Belgium ; (5) CEA, DSV, Institut de Radiobiologie Cellulaire et Moléculaire (iRCM), Laboratoire de recherche sur la Réparation et la Transcription dans les cellules Souches (LRTS), 18, route du Panorama, BP N° 6, 92265 Fontenay-aux-Roses cedex, France; (6) Centre Hospitalier Universitaire (CHU), Hopital de la Citadelle, B-4000 Liège, Belgium.

Running title: MT4-MMP alters tumor vessel architecture

*Corresponding author: A. NOEL: Laboratory of Tumor and Developmental Biology

University of Liège, Tour de Pathologie (B23)

Sart-Tilman, B-4000 Liège, BELGIUM

Tel: +32-4-366.25.69; Fax: +32-4-366.29.36

E-mail: agnes.noel@ulg.ac.be

ABSTRACT

The present study aims at investigating the mechanism by which MT4-MMP, a membrane-anchored MMP expressed by human breast tumor cells promotes the metastatic dissemination into lung. We applied experimental (intravenous) and spontaneous (subcutaneous) models of lung metastasis using human breast adenocarcinoma MDA-MB-231 cells overexpressing or not MT4-MMP. We found that MT4-MMP does not affect lymph node colonization nor extravasation of cells from the bloodstream, but increases the intravasation step leading to metastasis. Ultrastructural and fluorescent microscopic observations coupled with automatic computer-assisted quantifications revealed that MT4-MMP expression induces blood vessel enlargement and promotes the detachment of mural cells from the vascular tree, thus causing an increased tumor vascular leak. On this basis, we propose that MT4-MMP promotes lung metastasis by disturbing the tumor vessel integrity and thereby facilitating tumor cell intravasation.

INTRODUCTION

Several clinical and experimental investigations have indicated that breast cancer is an heterogeneous disease that could lead to a panel of proclivities, extending from a local disease to dissemination via lymphatic and/or hematogenous pathway [1]. A key feature of malignant cells is their ability to detach from the primary tumor and acquire migratory and invasive properties. To accomplish these goals, several proteolytic systems are used by cancer cells. The Matrix Metalloproteinases (MMPs) family of zinc dependent endopeptidases [2,3] represents one of the major protease families that have been associated with the progression of many cancers [4], including breast cancer [5,6], in which their role in tumor angiogenesis [7,8] and metastasis dissemination [9] has become evident. The MMP family includes secreted and membrane-anchored proteases [4]. Most of the Membrane Type-MMPs (MT-MMPs) are transmembrane proteases (MT1-, MT2-, MT3-, MT5-MMP) [10] but two members are exceptionally linked to the membrane by a glycosyl-phosphatidylinositol (GPI) anchor (MT4-, MT6-MMP) [11]. Discovered almost a decade ago, the function and the role of these GPI-MT-MMPs in cancer remain largely elusive when compared to other MT-MMPs.

MT4-MMP was originally cloned from a human breast carcinoma cDNA library [12,13] and has been detected in different organs including brain, colon, ovary, testis, uterus and lung [12-14]. The protein was also localized in inflammatory cells [11] and in several cancer cell lines [15] as well as in gliomas [16], prostate [17] and breast [12,18] carcinomas. MT4-MMP is unable to activate proMMP-2 and rather inefficient at hydrolyzing extracellular matrix (ECM) components compared to the other MT-MMPs [19]. Its catalytic domain is able to cleave *in vitro* very few substrates that include gelatin, fibrin(ogen), LRP, proTNF-alpha [19,20] and the aggrecanase ADAMTS-4 [21]. However, in MT4-MMP knock-out mice, neither proTNF-alpha shedding nor aggrecanalysis was affected by MT4-MMP depletion [14,22].

3

In a previous work, we demonstrated a higher immunostaining of MT4-MMP in breast cancer cells rather than in normal breast epithelial cells from human tissue samples [18]. Furthermore, the overexpression of MT4-MMP in the breast cancer cell line MDA-MB-231 enhanced subcutaneous tumor growth and most importantly led to lung metastasis when inoculated in RAG-1 immunodeficient mice [18]. However, no effect could be observed on proMMP-2 activation, VEGF production, angiogenesis nor cell migration and invasion *in vitro*. The unexpected tumor-promoting effect of MT4-MMP *in vivo*, together with its lack of effect on cancer cell invasion and proliferation *in vitro* suggest specific functions in the tumor microenvironment for this unconventional MT-MMP. Hence, to better understand the role of MT4-MMP, we applied histological methods and *in vivo* imaging to experimental (intravenous cell injection) or spontaneous (subcutaneous cell injection) models of metastasis. We provide evidence that MT4-MMP expression by cancer cells induce (i) an enlargement of blood vessels, (ii) a detachment of mural cells from the vascular tree and (iii) an increased tumor vascular leak. These effects of MT4-MMP promote hematogenous but not lymphatic dissemination of cancer cells by affecting the intravasation rather than the extravasation step of the metastatic cascade.

MATERIAL AND METHODS

Cell culture

Human breast cancer MDA-MB-231 cells were grown in Dulbecco's Modifed Eagle's Medium (DMEM) supplemented with 10% fetal calf serum (FCS), L-glutamine (2 mM), penicillin (100 U/ml) and streptomycin (100μg/ml) at 37°C in a 5% CO2 humid atmosphere. All culture reagents were purchased from Gibco-Life Technologies (Invitrogen Corporation, Paisley, Scotland). MDA-MB-231 cells stably expressing (MT4 clones) or not (CTR clones) MT4-MMP were obtained as previously described [18] by electroporation with pcDNA3-*neo* vector (Invitrogen) carrying the full-length human MT4-MMP cDNA or with a control empty vector, respectively. Three distinct clones stably expressing MT4-MMP and 3 control clones were maintained under basal pressure level of selection in medium containing 500 μg/ml of G418 (Life Technologies). For bioluminescent experiments, cells were transduced with lentiviruses encoding for firefly luciferase (Promega). Luciferase was checked to be expressed at same levels by incubation of cells in complete media supplemented with D-luciferin (150 μg/ml, Promega) and by bioluminescent observation using a PhotonImager camera system (Biospace, France).

Metastasis assays

Metastatic potential of MDA-MB-231 cells expressing or not MT4-MMP was investigated with two distinct models of metastasis in immunodeficient mice : (i) a "spontaneous" model of lung metastasis from a subcutaneous (s.c.) primary tumor and (ii) an "experimental" model in which lung metastasis were directly induced by intravenous (i.v.) injection of the tumor cells. In the spontaneous model, tumor cells $(1x10^6)$ were subcutaneously injected with matrigel (200 μl) in mice flank (n = 10) as previously described [18]. In the experimental metastasis model, cells were detached in PBS-EDTA 5 mM,

resuspended in serum-free medium (20×10^6 cells/ml) and injected (1×10^6 cells in 50 µl) into the lateral tail vein of the mice (n = 10). For each model of metastasis, either Rag-1 deficient mice or athymic nude mice (Charles River Laboratories, Lyon, France) were injected with tumor cells. Similar results were observed in both immunodeficient backgrounds. Metastases were detected 6 or 8 weeks after injection by histological, *in vivo* or *ex vivo* bioluminescence analyses.

For histological analyses, paraffin-embedded organs were cut at 5 µm-thick and metastasis were detected by immunostaining for human Ki-67 protein as previously described [18]. The metastatic foci were counted in 45 histological fields per section at 200-fold magnification. The incidence of metastasis defines the percentage of mice with detectable Ki-67 positive metastatic cells in the lung. The severity of metastasis characterizes the size of metastatic foci (number of Ki-67 positive cells per foci).

For *in vivo* bioluminescence imaging of metastasis, nude mice were anesthetized with isofluorane (1-3%) and injected intraperitonealy with D-luciferin (Promega ; 150 mg/kg in PBS). Mice were then placed onto a warmed stage inside the light-tight camera box with continuous exposure to 1–2% isoflurane. Five mice were imaged at a time for 1-5 min of exposition to a PhotonImager optical camera (Biospace Lab, France). For *ex vivo* imaging, mice were sacrificed and tissues of interest were excised, placed into 24-well tissue culture plates containing D-luciferin (300 µg/ml in PBS) and imaged for 2 min.

Lung extravasation assay

In order to assess the short-term extravasation of cells to the lungs of mice, cells were incubated for 30 min at 37°C in serum-free DMEM with 2.5 µM of red-fluorescent CMTPX CellTracker (Invitrogen, Molecular Probes, C34552), washed and reincubated in fresh serum-free DMEM for another 30 min before being intravenously injected in nude mice as described

above (n = 10). After 48 hrs, mice were anesthetized by intraperitoneal injection of Nembutal (200 µl / mice) and their vasculature was labelled (modified protocol from [23]) by intracardiac injection of (FITC)-labelled *Lycopersicon Esculentum* (tomato) lectin (100 µg in 100 µl 0.9% NaCl, Vector Laboratories, Burlingame, CA, FL-1171) which was allowed to circulate for 5 minutes. The pulmonary vasculature was then fixed by perfusion of 20 ml of paraformaldehyde 4% / PBS (PFA) through the right ventricle during 2 minutes whereas the blood / fixative mix was allowed to escape out of the lung vascular network by a small incision in the left atrium. Lungs were then harvested, fixed in 4% PFA at 4 °C for 1 hr, incubated in sucrose 30% / azide 0.1% / PBS at 4°C overnight, rinsed in PBS, frozen embedded in OCT compound (Tissue-Tek) and cut at 6 µm-thick with cryostat. Frozen sections were washed 3 times in PBS for 5 min, then dried at room temperature for 15 minutes, counterstained and mounted with Vectashield Medium with DAPI (Vector Laboratories, Burlingame, CA, H-1200). FITC lectin-labelled vasculature was then analyzed by fluorescence microscopy at 400-fold magnification. Red CMTPX-labelled tumor cells remaining in the lungs after the perfusion were considered as extravasating tumor cells and counted in 20 microscopic optical fields.

Histological and functional analysis of tumor lymphatic vessels

Six weeks post cancer cell injection, tumor lymphatic vessels were visualized by immunostaining of 5-µm thick paraffin sections of xenografts using an anti-LYVE-1 rabbit polyclonal antibody (Upstate USA, Inc, Charlottesville, VA, ref. 07-538). To unmask antigens, slides were autoclaved for 11 min at 126°C in Target Retrieval Solution (Dako, S1699). Endogenous peroxidase was blocked by 3% H_2O_2 / H_2O for 20 min and non-specific binding was prevented by incubation in PBS / BSA 10% (Fraction V, Acros Organics, NJ) for 1 hr. Sections were then incubated with the anti-LYVE-1 antibody (1:1000) for 1 hr, with a

biotinylated second antibody (Dako, E0432, 1:400) for 30 min and then with a Strepatavidin / HRP complex (Dako, P0397, 1:500) for 30 min. Slides were then coloured with 3-3'diaminobenzidine hydrochloride (DAB, Dako, K3468), counter-stained with hematoxylin and mounted with Eukitt medium for microscope observation.

For functional assessment of tumor lymphatic network and for *in vivo* visualization of sentinel lymph nodes [24] of xenografted mice (n = 5), semiconductor fluorescent nanocrystal Quantum Dots (Qdot® 705 ITK™, Invitrogen, Molecular Probes, ref. Q21561MP) were used. Mice bearing tumors were anesthetized with isofurane (1-3%) and 10 µl of Qdots (8 µM) were directly injected into the tumors. Drainage of Qdots from the tumor to sentinel lymph nodes was visualized 24 hours after Qdots injection by fluorescent imaging using a PhotonImager optical camera.

Ultrastructure of tumor vasculature by transmission electron microscopy

Tumor xenografts excised at day 30 post cell injection in Rag-1 deficient mice were fixed for 1 hour at 4°C with 2.5% glutaraldehyde in a Sörensen 0.1 M phosphate buffer (pH 7.4). After postfixation for 30 minutes with 1% osmium tetroxide and deshydratation, samples were embedded into Epon (Luft, 1961). Ultrathin sections obtained with a Reichert Ultracut S ultramicrotome were contrasted with uranyl acetate and lead citrate. Observations were done with a Jeol 100 CX II transmission electron microscope at 60 kV.

Analysis of tumor vaculature by fluorescent microscopy

Mice bearing tumors were euthanized between 4 and 6 weeks (in order to standardize the tumor volumes) after s.c. tumor cell injection. Functional tumor vasculature was visualized by intravenous injection of (FITC)-labelled *Lycopersicon Esculentum* (tomato) lectin and the vascular tree was maintained in an open state by perfusion with PFA as

described above excepting the following modifications: the vasculature was fixed by perfusion of 40 ml of PFA (120 mm Hg), for 4 minutes via the left ventricle and the blood-exit incision was performed in the right atrium. Tumors were then harvested, fixed in 4% PFA at 4°C for 24 hrs, incubated in sucrose 30% / azide 0.1% / PBS at 4°C for 48 hrs, rinsed in PBS, embedded and frozen in OCT compound (Tissue-Tek).

To visualize perivascular cells, thick frozen sections (100 μm) were rinsed in PBS, permeabilized in PBS / 0.3% Triton X-100 / 0.25% gelatin for 30 min at room temperature and incubated for 2 hrs in the permeating solution containing Cy3-conjugated mouse monoclonal antibody raised against anti-alpha-smooth muscle actin (SMA) (1:1,000, clone 1A4, C6198, Sigma). Sections were then washed in PBS and mounted with Vectashield Hard Set Medium with DAPI (Vector Laboratories, Burlingame, CA, H-1400) for fluorescence microscopic observations.

Vascular morphometric measurements

Thick sections of xenografts expressing (n = 10) or not (n = 5) MT4-MMP were observed with a fluorescent microscope (Olympus) at 200-fold magnification. The whole surface of tumor sections was scanned and photomicrographed (50-100 / section). The mean vessel density was calculated by counting the number of intratumor blood vessels present either on the whole area sections or on the most vascularised area ("hot spots") of the sections. The cross-sectioned area and the size distribution of the blood vessels were analyzed using ImageJ software (http://rsb.info.nih.gov/ij/). According to previous studies [23,25], one of the following diameter categories was assigned to each vessel : < 25 μm (small), between 25 μm - 50 μm (medium) or ≥ 50 μm (large).

In order to analyze the mural cells distribution around the blood vessels, an original computer-assisted quantification was developed by implementing an algorithm in MATLAB

software (http://www.mathworks.com/): concentric rings were drown all around the vessels by successive dilatation of vessels shape at similar intervals of distance. The densities of red pixels (mural cells) crossed by this grid were then calculated as a distance function from the green pixels (endothelial cells). Although the grids shown in figure 4 are simplified for a better visibility, the grids used for the quantifications were drawn at 3 concentric rings/µm.

Evaluation of tumor vascular leakage

Six weeks post tumor cell injection, xenografted nude mice (n = 3) were anesthetized with isofurane (1-3%) and intravenously injected with 150 µl (2 mM in PBS) of AngioSense™ 680 vascular probe (VisEn Medical Inc, Woburn, MA, USA). Fluorescent signal of AngioSense was monitored in the mice 7 hours and 24 hours after the probe administration using a PhotonImager camera. Region of interest (ROI) were drawn on the tumour and a reference zone in the abdomen in order to measure the fluorescence intensity (cpm/mm2). The vascular leak in the tumour was quantified as the ratio fluorescence from the tumour / fluorescence from the reference.

Statistical analysis

Statistical differences between experimental groups were assessed using the non parametric Mann-Whitney test in which P-values < 0.05 (*) were considered as significant. Statistical analyses were carried out using Prism 5.0 software (GraphPad, San Diego, CA).

RESULTS

MT4-MMP over-expression does not affect lymph node metastasis

MT4-MMP overexpression in MDA-MB-231 cells has been previously associated with higher levels of lung metastases when subcutaneously injected into mice [18]. In order to determine whether this pro-metastatic effect of MT4-MMP could be related or associated to a higher lymphatic tumor cell dissemination, the presence of lymphatic vessels in the xenografts was first analysed by LYVE-1 immunostaining (Fig. 1 A, left panels). While some LYVE-1 positive lymphatic vessels were detected in the xenografts, mainly at the periphery of the tumor, no difference was evidenced between xenografts expressing or not MT4-MMP. The functionality of lymphatic vessels was then assessed by analysing the lymphatic drainage of fluorescent Quantum Dots (Qdot), 24 hours after their intratumoral injection (Fig 1 A, middle and right panels). A rapid and reproducible migration of fluorescent nanoparticules was observed in sentinel lymph nodes of mice. However, these nanocristals accumulated in regional (inguinal) and distal (axillary) lymph nodes independently of MT4-MMP status (Fig. 1 A, right panels).

To confirm by bioluminescence imaging (BLI) that MT4-MMP promotes lung metastasis from subcutaneous grafts, cells expressing MT4-MMP and luciferase or their control clones have been generated (Fig. 1 B and Fig. 2 A). We checked by RT-PCR and Western blot that luciferase expression did not affect MT4-MMP production (data not shown). Due to the high bioluminescence signal from the primary tumour, weak bioluminescence signal from micro-metastases were difficult to access directly *in vivo*. Therefore *ex vivo* analyses were also performed on lymph nodes and lungs recovered 8 weeks after subcutaneous injection of cancer cells (Fig. 1 B). Lung metastasis was clearly increased after the injection of cells expressing MT4-MMP compared with control cells (60 % versus 0 %) (Fig. 1 B). However, no significant difference in the incidence of lymph node metastasis

was observed between MT4-MMP expressing or control cells (Fig. 1 B). Altogether, these data suggest that MT4-MMP expression improves lung metastasis but not lymphatic dissemination.

MT4-MMP over-expression does not affect extravasation from the blood to the lungs

To distinguish between an effect on primary invasion (fater subcutaneous injection) and extravasation from the bloodstream, cells expressing MT4-MMP and luciferase or their controls were alternatively injected via the tail vein. In these conditions, in sharp contrast to the xenograft model (Fig. 2 A), the percentage of animals with lung colonies was not influenced by MT4-MMP expression (100 % versus 80 % with MT4-MMP expressing or control cells, respectively) (Fig 2 C).

To assess the histological severity of lung metastasis, Ki-67 immunostaining were performed on lung sections to detect human metastatic cells (Fig. 2 B, D) [18]. Metastatic nodules were scored according to the number of Ki-67 positive cells: severity-1 (< 3 cells), severity-2 (between 3 and 20 cells), severity-3 (>20 cells). As previously reported [18], the severity of metastasis was drastically increased by MT4-MMP expression after subcutaneous injection (Fig 2 B). In sharp contrast, after intravenous cell inoculation, neither the number nor the severity of lung metastasis was affected by MT4-MMP expression (Fig. 2 D).

We have then evaluated the ability of cells to adhere and extravasate from blood vessels into the lungs of mice in a short-term assay. After intravenous injection of cells pre-labelled with a red-fluorescent cell tracker (n = 10), lung vasculature was visualized 48 hours latter by perfusion with a FITC-conjugated lectin. Remaining adhering / extravasating tumor were detected in the lung of 100 % mice and no difference was observed between mice injected with MT4-MMP expressing cells (MT4 clones) or control cells (CTR clones) (Fig. 2

E). All these data support the notion that MT4-MMP does not affect the extravasation efficiency of cancer cells to the lungs.

MT4-MMP over-expression affects intratumoral blood vessel size and perivascular cell distribution

We next investigated the primary tumor vascular architecture by transmission electron and fluorescent microscopic analysis. As opposed to similarities in the ultrastructural features of endothelial cells, explicit differences were noted between the two experimental groups with regard to endothelial cell and pericyte interactions. As previously described in other types of tumors [23,25], basement membranes wrapping around tumor pericytes were abnormally thick, irregular and sometimes absent in both experimental conditions (data not shown). However, pericytes of xenografts expressing MT4-MMP were irregularly shaped, extended cytoplasmic processes and were loosely associated with endothelial cells (Fig. 3 A) in comparison with those of control xenografts which were apposed to endothelial cells (Fig. 3 B). Interestingly, intravasation of tumor cells were observed in MT4-MMP expressing xenografts, in which tumor cells extended protrusions into the lumen of vessels (in 3 out of 25 vessels observed)(Fig. 3 C). In contrast, in control xenografts, intravasation process was never detected and their vessels displayed a thick intact basement membrane supporting apposed endothelial (Fig. 3 D).

Functional vascular tree of subcutaneous xenografts was then analysed by fluorescent microscopic observation of thick tumor sections. Tumor vessels washed free of blood were visualized by intraluminal staining with a FITC-conjugated lectin and perivascular cells were immunostained for alpha smooth muscle actin (SMA). Xenografts expressing MT4-MMP were characterized by enlarged blood vessels (Fig. 4 B) compared with control xenografts (Fig. 4 A). To determine the distribution of blood vessel size, one of the following size

categories was assigned to each vessel according to their diameter: < 25 μm (small), between 25 μm - 50 μm (medium) or ≥ 50 μm (large). In MT4-MMP tumors compared to control xenografts, the percentage of small vessels fell from 78 % to 58 % ($P < 0.05$) while those of medium and large-sized vessels rose from 18 % to 29 % ($P < 0.05$) and from 4 % to 13 % ($P < 0.01$) (Fig. 4 C). The density of large vessels was 2-fold higher ($P = 0.01$) in tumors expressing MT4-MMP as compared to control tumors (data not shown) whereas no significant difference in the total blood vessel density was observed between both conditions as assessed by quantification of the total number of vessels either present on the whole tumor section (Fig. 4 D) or on "hot spots" tumor areas (data not shown). However, an increase of the mean cross-sectioned blood vessel area ($P = 0.002$) was noticed in MT4-MMP expressing xenografts (Fig. 4 E). This vascular enlargement further confirms the effect of MT4-MMP expression on vessel architecture rather than on vascular density.

In order to quantify the detachment of pericytes observed in the enlarged vessels of tumor expressing MT4-MMP (Fig. 4 A, B), we set up a computer-assisted quantification using a grid of SMA-positive cell distribution (Fig. 4 A, B ; right upper corners). More than 800 and 400 blood vessels from 10 MT4-MMP-expressing and 5 control xenografts, respectively, were analyzed. Perivascular cell distribution calculated as a distance function from the tumor blood vessels, shows that the density of "detached" mural cells present at 5 μm, 10 μm or 15 μm from endothelial cells were 2-folds higher in MT4-MMP expressing tumors compared to control xenografts (Fig. 4 F). These data reflect impaired pericytes-endothelial cells interactions which is consistent with the transmission electron and fluorescent microscopic observations.

MT4-MMP effect on blood vessel morphology is associated with an increase of vessel leakage

In order to verify whether the strong effect of MT4-MMP on blood vessel architecture could increase the permeability of vessels, we have used AngioSense680 vascular probe which is a fluorescent polymeric macromolecule of 250 kD. Due to its high molecular size, this probe remains in the blood for a long time and can extravasate into tissues containing blood vessels that have large gaps between endothelial cells. This phenomenon, called "Enhanced Permeability and Retention" (EPR) effect, is well known to target tumour containing leaky blood vessels [26,27]. This probe was therefore used to assess *in vivo* vascular leak of blood vessels in the xenografts expressing or not MT4-MMP. Seven hours after its intravenous injection, the AngioSense680 was uniformly distributed in the vasculature of all mice bearing tumors and no difference of fluorescence could be observed between xenografts either expressing or not MT4-MMP (Fig. 5 A and C). However, 24 hours after injection, the probe had extravasated and strongly accumulated in tumor areas of MT4-MMP expressing xenografts compared to the control xenografts (Fig. 5 B and C).

DISCUSSION

The direct implication of MMPs in tumor progression is extensively documented and an increasing number of evidences shows that MMP could have a much broader role in the metastatic process than initially expected, including their intervention in key steps of the metatastatic cascade such as angiogenesis, intravasation, extravasation and initiation/maintenance of secondary tumor growth [9,28,29]. However, to date, very few MMPs (MMP-7, MMP-8, MT1-MMP, MT4-MMP) have been described to directly modulate the dissemination of cancer cells at distance from a primary tumor, as assessed in spontaneous models of metastasis (subcutaneous xenografts) [18,30-32]. Moreover their mechanisms of action and the specific steps of the metastatic cascade affected by these MMPs are unknown.

In the present study, by using different approaches of immunohistological, ultrastructural and *in vivo* imaging analyses, we provide evidence that the pro-metastatic effect of MT4-MMP occurs by affecting the hematogenous route of tumor cell spreading rather than the lymphatic way. Indeed, we demonstrate that MT4-MMP does not affect the incidence of lymph node metastasis nor the functionality of tumor lymphatic network. In contrast, the overexpression of MT4-MMP led to higher spontaneous but not experimental lung metastasis. It did not detectably affect tumor cell extravasation or early implantation into lung but increased the hematogenous dissemination of tumor cells from a primary subcutaneous tumor. Thus, MT4-MMP affects more likely the intravasation process than later steps of the metastatic dissemination. In agreement with previous reports, intravasation is described as one of the rate-limiting steps of the metastatic process [9,33] while extravasation is qualified as a rather efficient process [28,34]. This impact of MT4-MMP on metastasis could not be ascribed to a clonal effect since similar results were obtained by using 3 different clones over-expressing MT4-MMP [18]. In addition, in the present study, the generation of

16

cells expressing luciferase gave rise to similar promoting effect on the metastatic dissemination, without affecting MT4-MMP production.

Vascular architecture of primary tumors expressing or not MT4-MMP was explored by transmission electron and fluorescent microscopy. Although MT4-MMP expression in xenografts did not affect the total blood vessel density, it was associated with an enlargement of intratumor blood vessels with an increase of the mean vessel cross-sectioned area and the density of large vessels. Interestingly, a detachment of mural cells from the endothelial cells as well an increase of macromolecules leakage was detected in the tumors expressing MT4-MMP. Based on these findings, the metastasis promoting effect of MT4-MMP could be explained by its effects on blood vessel architecture making them more permissive to tumor cells intravasation. This is consistent with the observations of intravasating tumor cells in xenografts expressing MT4-MMP by electron transmission microscopy. Hence, the larger, destabilized and leaky blood vessels observed in xenografts expressing MT4-MMP could lead to a higher level and a more efficient intravasation of tumor cells into the blood vasculature. In agreement with this concept, a relation between the blood vessel architecture and the development of metastasis has been reported. Mouse models with deficiencies in pericytes / endothelial cells interactions [35,36] and genetic engineered mice with blood vessel structural fragilities [37] develop more hematogenous metastasis. The presence of pericytes and their interaction with endothelial cells are thought to limit tumor metastatic dissemination as demonstrated by studies using mouse tumor models with loss / gain of NCAM or PDGF-B lacking the motif necessary to its endothelial retention [35,36]. Therefore, this study reports for the first time, the implication of MT4-MMP in tumor cell intravasation and its effect on blood vessels integrity. Such a novel role for MT4-MMP in tumor blood vessel architecture is consistent with its expression in various smooth muscle cells [14] or in endothelial and perivascular cells of human endometrium *in vitro* [38] and *in vivo* during menstrual phases

associated with high angiogenic activities [39]. Our paper sheds light on the contribution of MT4-MMP in metastatic dissemination in agreement with the relationship recently established between MT4-MMP expression and the transition from pre-invasive to invasive breast cancer [40].

Given the importance of the ECM deposition in blood vessel formation / stabilization and the broad range of ECM substrates cleaved by MMPs [3,4], it is not surprising that one of theses proteases could affect tumor blood vessel morphology. However, MT4-MMP is one of the lest efficient MMPs toward ECM protein degradation and its catalytic domain is unable to cleave important blood vessel basement membrane components such as type-IV collagen, fibronectin, laminin and decorin [19, 41, 42]. Nevertheless, new functions recently emerged for MMPs including their involvement in pericytes recruitment [43] through (i) a mobilization of bone marrow derived progenitors [44], (ii) a regulation of vessel wall architecture by modulating PDGF-B / PDGFRβ signaling pathway [45] and/or (iii) an alteration of pericyte adhesion. For instance, MT1- and MT3-MMP are able to decrease the integrin-mediated cell adhesion by cleaving focal adhesion kinases in vascular smooth muscle cells [46]. However, in our study, MT4-MMP expressed by cancer cells did not affect their adhesion *in vitro* to different matrices including laminin, fibronectin, type-I collagen, gelatin, endothelial cells layer or their ECM deposit (data not shown). MT4-MMP could affect vessel integrity through different mechanisms. For instance, it could contribute to the shedding of molecules more specifically implicated in pericytes / endothelial cells adhesion as it has been demonstrated for other MMPs [3,47]. In order to determine the impact of MT4-MMP on endothelial cell differentiation and/or endothelial cell to pericyte interactions, monocultures, as well as co-cultures of these different cells types including tumour cells or medium conditioned by tumour cells were performed on matrigel. All these *in vitro* attempts failed to reproduce the *in vivo* observations. This fits with our previous work showing that MT4-MMP production did

not affect tumour cell properties *in vitro* [18]. These information suggest that MT4-MMP exerts its effect through cellular or extracellular factor(s) present in the tumour microenvironment, but absent *in vitro*. In an attempt to elucidate the molecular mechanisms of MT4-MMP action, we have searched for modulation of the levels of different major angiogenic regulators in xenografts expressing or not MT4-MMP (data not shown). Neither VEGF, ANG-1, ANG-2, TIE-1, TIE-2, NRP-1, PDGF-B, PDGFR-B, HGF, AKT-1, PAI-1, MMP-2, MMP-9, MT1-MMP nor PECAM mRNA levels were affected by MT4-MMP expression as assessed by RT-PCR analyses (data not shown). In addition, no difference in the production of key angiogenic modulators (VEGF, PDGFR, FGF and their receptors) was detected at the protein levels by antibodies arrays. However the mRNA expression of human thrombospondin-2 was 3-fold decreased in xenografts expressing MT4-MMP compared to control xenografts ($P = 0.002$) (data not shown). Interestingly, a reduced expression of this antiangiogenic factor has already been associated with impairment of vascular integrity and permeability in mouse models [48] and its genetic deletion in TSP-2 knock-out mice favors tumor growth, metastasis and angiogenesis [49,50]. Altogether, these data suggest that the downregulation of TSP-2 expression observed upon MT4-MMP production could, at least partly, account for the impairment of the vascular integrity and thereafter for the increased metastatic dissemination.

In conclusion, during the last decade, the contribution of various MMPs to both early and late events of the metastatic process has emerged. However, the role of GPI-anchored MT-MMP has been shadowed by a focus on soluble MMPs and MT1-MMP. The present results provide evidence for an implication of the GPI-anchored MT4-MMP in the intravasation rather than in the extravasation step of metastatic process, through the disruption of vascular integrity in primary tumors. It also underlies the impact of MT4-MMP on hematogenous, but not lymphatic spread.

ACKNOWLEDGMENTS

FIGURE LEGENDES

Figure 1. *Effect of MT4-MMP on tumor lymphatic network and lymph node metastasis.* The tumor lymphatic network (***A***) and the presence of lymph node metastasis (***B***) were analysed in athymic nude mice after subcutaneous injection of MDA-MB-231 breast cancer cells expressing (*MT4-xenografted mice ; upper panels*) or not (*CTR-xenografted mice ; lower panels*) MT4-MMP. ***A :*** Lymphatic vessels were detected at the interface between the tumors (*T*) and the host stroma (*S*) by LYVE-1 immunostaining of xenograft sections (*left panel*). Functionality of tumor lymphatic network was assessed by lateral (*middle panel*) and ventral (*right panel*) visualization of sentinel lymph nodes 24 hours after intratumoral injection of fluorescent nanocrystals (*Qdot*). Black arrows indicate accumulated Qdot particules in the regional (*inguinal ; I*) and distal (*axillary ; A*) lymph nodes. ***B :*** The presence of regional (*inguinal ; I*) and distal (*axillary ; A*) lymph node (*LN*) metastases as well as lung metastases were detected by bioluminescent analysis of the luciferase reporter gene in each organ *ex vivo*. Percentage represents the incidence of mice with detectable metastasis in each organ (n=10).

Figure 2. *Effect of MT4-MMP on lung metastases.* MDA-MB-231 breast cancer cells expressing (*MT4 clones*) or not (*CTR clones*) MT4-MMP were injected into immunodeficient mice either subcutaneously (*spontaneous model of metastasis : **A** and **B***) or intravenously (*experimental model of metastasis : **C, D** ; **E***). ***A-D :*** After 6 weeks of incubation, subcutaneously- (***A, B***) and intravenously- (***C, D***) injected mice were analysed for the presence of lung metastases by *in vivo* bioluminescent detection of luciferase reporter gene (***A, C***) and by histological analyses of lung sections after Ki-67 immunostaining (***B, D***). ***A, C***: numbers represent the percentage of mice with lung metastases. ***B, D:*** Severity of metastasis was determined by counting Ki-67 positive cells in metastatic foci and scored as: severity-1 (less than 3 stained cells), severity-2 (3 to 20 cells) or severity-3 (more than 20 stained cells)

(***B, C***). ***E :*** Cells pre-labelled with red-fluorescent CMTPX Cell Tracker were intravenously injected. After 48 hours, extravasating cells *(in red)* from the FITC-lectin-labelled blood vessels (*in green*) were analysed by fluorescent microscopic observation of lung sections counterstained with DAPI (*in blue*) (scale bar = 50 µm). The number of tumor cells was counted on 20 microscopic fields (X400). Results are expressed as the mean of each experimental group (n=10). Error bars represent SE. *$P < 0.05$; ***$P < 0.001$.

Figure 3. *Transmission electron micrographs of blood vessels in breast cancer xenografts.* Transfectants were subcutaneously injected into Rag-1 immunodeficient mice. After 4 weeks of incubation, ultrathin sections of xenografts expressing (*Xenograft MT4*; ***A, C***) or not (*Xenograft CTR* ; ***B, D***) MT4-MMP were analyzed with a Jeol 100 CX II transmission electron microscope at 60 kV. ***A, B:*** Pericytes *(p) are* present in both conditions but are irregularly shaped, extend more frequent cytoplasmic processes (*black arrows*) and are loosely associated with endothelial cells (*ec*) in tumors expressing MT4-MMP (***A***) compared to control tumors (***B***). ***C, D:*** Intravasating tumor cells (*black arrow-head*) were preferentially observed in the lumen (*l*) of blood vessels of xenografts expressing MT4-MMP (***C***) in contrast with control xenografts where tight associations between endothelial cells (*ec*) were observed (***D***). *Rc*, red blood cell. *A and B* at 8,000-fold magnification (scale bar = 2 µm). *C* and *D* at 13,000-fold magnification (scale bar = 1 µm).

Figure 4. *Effect of MT4-MMP on tumor blood vessel morphology and perivascular cells distribution.* Functional vascular tree of xenografts expressing or not MT4-MMP was visualized by intravenous injection of a (FITC)-labelled lectin in tumor-bearing mice (n = 10). ***A, B****:* Fluorescent photomicrographs of representative sections of xenografts expressing (***A***) or not (***B***) MT4-MMP and showing an enlargement of FITC-lectin-labelled blood vessels (*in*

green) as well as alpha-SMA positive mural cells (*in red*) distribution around the vessels (scale bar = 100 μm). ***C, D, E:*** The diameter, the density and the area of blood vessels (*vsls*) of thick tumor sections from xenografts expressing (*black histograms*) or not (*white histograms*) MT4-MMP were assessed using ImageJ software. ***C :*** The distribution of the lumen of tumor blood vessels is expressed as the percentage of blood vessels observed on the whole tumor sections according to the respective diameter categories (small : < 25 μm ; medium : ≥ 25 μm and < 50 μm ; large : ≥ 50 μm). ***D***: Mean blood vessel density observed on the on the highest vascularised regions (*hotspots*). ***E:*** Mean size of the blood vessels assessed by measurement of their cross-sectioned area (*mean area/vsl*). Error bars represent SE. *$P < 0.05$; **$P < 0.01$. ***F:*** Perivascular cells distribution in function of the distance from the tumor blood vessels. The pixel density of alpha-SMA positive cells at 5 μm from endothelial cells is still 2-folds higher in MT4-MMP condition (*black squares*) compared to control condition (*white squares*). Examples of quantification grids used to measure the perivascular cell distribution are shown in the right upper corners of photomicrographs ***A*** and ***B***.

Figure 5. *Vascular leakage of breast cancer xenografts expressing MT4-MMP*. The vascular permeability of subcutaneous xenografts expressing (*MT4*) or not (*CTR*) MT4-MMP was assessed by injecting intravenously a fluorescent probe AngioSense™ 680 (n=5). ***A, B :*** Representative distribution of fluorescent macromolecule remaining in the mice 7 hours (***A***) and 24 hours (***B***) after intravenous administration. Tumors are delineated by dotted circle. ***C:*** Quantification of fluorescence ratio tumour / surrounding abdominal tissue. Error bars represent SE. **$P < 0.01$.
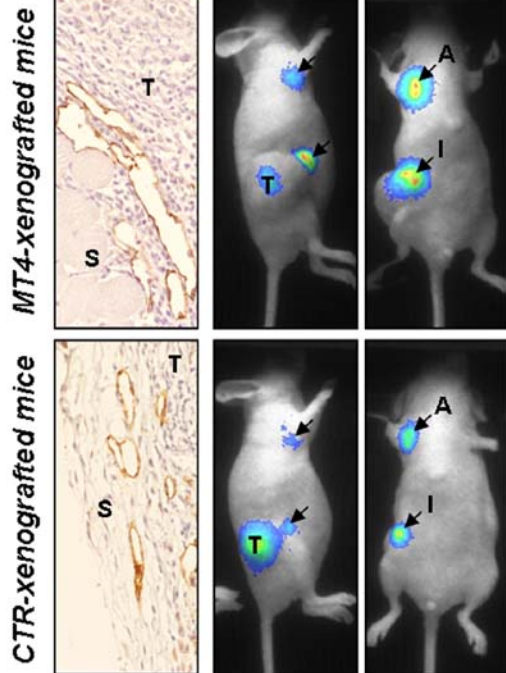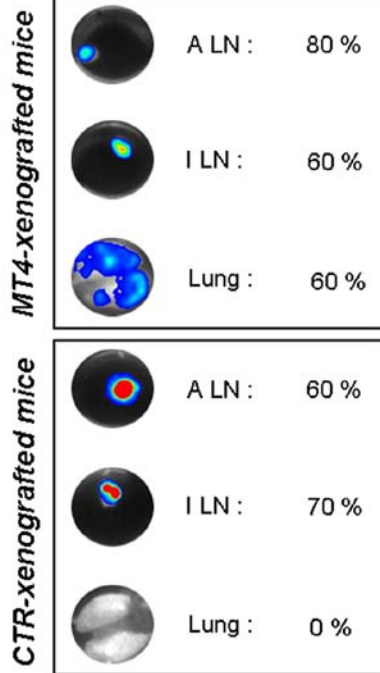
REFERENCES

[1] **Cady B.** Regional lymph node metastases; a singular manifestation of the process of clinical metastases in cancer: contemporary animal research and clinical reports suggest unifying concepts. *Ann. Surg. Oncol.* 2007; 14: 1790-1800.

[2] **Folgueras AR, Pendas AM, Sanchez LM, Lopez-Otin C.** Matrix metalloproteinases in cancer: from new functions to improved inhibition strategies. *Int. J Dev. Biol.* 2004; 48: 411-24.

[3] **Cauwe B, Van den Steen PE, Opdenakker G.** The biochemical, biological, and pathological kaleidoscope of cell surface substrates processed by matrix metalloproteinases. *Critical Reviews in Biochemistry and Molecular Biology.* 2007; 42: 113-85.

[4] **Egeblad M, Werb Z.** New functions for the matrix metalloproteinases in cancer progression. *Nature Reviews Cancer.* 2002; 2: 161-74.

[5] **Chabottaux V, Noel A.** Breast cancer progression: insights into multifaceted matrix metalloproteinases. *Clin. Exp. Metastasis.* 2007; 24: 647-56.

[6] **Chabottaux V, Noel A.** Matrix metalloproteinases to predict breast cancer metastases. *Clin. Lab. Int.* 2007; 31: 8-10.

[7] **Handsley MM, Edwards DR.** Metalloproteinases and their inhibitors in tumor angiogenesis. *Int. J. Cancer.* 2005; 115: 849-60.

[8] **van Hinsbergh VW, Koolwijk P.** Endothelial sprouting and angiogenesis: matrix metalloproteinases in the lead. *Cardiovasc. Res.* 2008; 78: 203-12.

[9] **Deryugina EI, Quigley JP.** Matrix metalloproteinases and tumor metastasis. *Cancer Metastasis Rev.* 2006; 25: 9-34.

[10] **Sounni NE, Noel A.** Membrane type-matrix metalloproteinases and tumor progression. *Biochimie.* 2005; 87: 329-42.

[11] **Sohail A, Sun Q, Zhao H, Bernardo MM, Cho JA, Fridman R.** MT4-(MMP17) and MT6-MMP (MMP25), A unique set of membrane-anchored matrix metalloproteinases: properties and expression in cancer. *Cancer Metastasis Rev.* 2008; 27: 289-302.

[12] **Puente XS, Pendas AM, Llano E, Velasco G, Lopez-Otin C.** Molecular cloning of a novel membrane-type matrix metalloproteinase from a human breast carcinoma. *Cancer Res.* 1996; 56: 944-9.

[13] **Kajita M, Kinoh H, Ito N, Takamura A, Itoh Y, Okada A, Sato H, Seiki M.** Human membrane type-4 matrix metalloproteinase (MT4-MMP) is encoded by a novel major transcript: isolation of complementary DNA clones for human and mouse mt4-mmp transcripts. *FEBS Lett.* 1999; 457: 353-6.

[14] **Rikimaru A, Komori K, Sakamoto T, Ichise H, Yoshida N, Yana I, Seiki M.** Establishment of an MT4-MMP-deficient mouse strain representing an efficient tracking

system for MT4-MMP/MMP-17 expression in vivo using beta-galactosidase. *Genes Cells.* 2007; 12: 1091-100.

[15] **Grant GM, Giambernardi TA, Grant AM, Klebe RJ.** Overview of expression of matrix metalloproteinases (MMP-17, MMP-18, and MMP-20) in cultured human cells. *Matrix Biol.* 1999; 18: 145-8.

[16] **Nuttall RK, Pennington CJ, Taplin J, Wheal A, Yong VW, Forsyth PA, Edwards DR.** Elevated membrane-type matrix metalloproteinases in gliomas revealed by profiling proteases and inhibitors in human cancer cells. *Mol. Cancer Res.* 2003; 1: 333-45.

[17] **Riddick AC, Shukla CJ, Pennington CJ, Bass R, Nuttall RK, Hogan A, Sethia KK, Ellis V, Collins AT, Maitland NJ, Ball RY, Edwards DR.** Identification of degradome components associated with prostate cancer progression by expression analysis of human prostatic tissues. *Br. J. Cancer.* 2005; 92: 2171-80.

[18] **Chabottaux V, Sounni NE, Pennington CJ, English WR, van den Brule F, Blacher S, Gilles C, Munaut C, Maquoi E, Lopez-Otin C, Murphy G, Edwards DR, Foidart JM, Noel A.** Membrane-type 4 matrix metalloproteinase promotes breast cancer growth and metastases. *Cancer Res.* 2006; 66: 5165-72.

[19] **English WR, Puente XS, Freije JM, Knauper V, Amour A, Merryweather A, Lopez-Otin C, Murphy G.** Membrane type 4 matrix metalloproteinase (MMP17) has tumor necrosis factor-alpha convertase activity but does not activate pro-MMP2. *J. Biol. Chem.* 2000; 275: 14046-55.

[20] **Rozanov DV, Hahn-Dantona E, Strickland DK, Strongin AY.** The low density lipoprotein receptor-related protein LRP is regulated by membrane type-1 matrix metalloproteinase (MT1-MMP) proteolysis in malignant cells. *J. Biol. Chem.* 2004; 279: 4260-8.

[21] **Gao G, Plaas A, Thompson VP, Jin S, Zuo F, Sandy JD.** ADAMTS4 (aggrecanase-1) activation on the cell surface involves C-terminal cleavage by glycosylphosphatidyl inositol-anchored membrane type 4-matrix metalloproteinase and binding of the activated proteinase to chondroitin sulfate and heparan sulfate on syndecan-1. *J. Biol. Chem.* 2004; 279: 10042-51.

[22] **Stewart MC, Fosang AJ, Bai Y, Osborn B, Plaas A, Sandy JD.** ADAMTS5-mediated aggrecanolysis in murine epiphyseal chondrocyte cultures. *Osteoarthritis. Cartilage.* 2006; 14: 392-402.

[23] **Hashizume H, Baluk P, Morikawa S, McLean JW, Thurston G, Roberge S, Jain RK, McDonald DM.** Openings between defective endothelial cells explain tumor vessel leakiness. *Am. J. Pathol.* 2000; 156: 1363-80.

[24] **Ballou B, Ernst LA, Andreko S, Harper T, Fitzpatrick JA, Waggoner AS, Bruchez MP.** Sentinel lymph node imaging using quantum dots in mouse tumor models. *Bioconjug. Chem.* 2007; 18: 389-96.

[25] **Morikawa S, Baluk P, Kaidoh T, Haskell A, Jain RK, McDonald DM.** Abnormalities in pericytes on blood vessels and endothelial sprouts in tumors. *Am. J. Pathol.* 2002; 160: 985-1000.

[26] **Maeda H, Wu J, Sawa T, Matsumura Y, Hori K.** Tumor vascular permeability and the EPR effect in macromolecular therapeutics: a review. *J. Control Release.* 2000; 65: 271-84.

[27] **Greish K.** Enhanced permeability and retention of macromolecular drugs in solid tumors: a royal gate for targeted anticancer nanomedicines. *J. Drug Target.* 2007; 15: 457-64.

[28] **Chambers AF, Groom AC, MacDonald IC.** Dissemintation and growth of cancer cells in metastatic sites. *Nat. Rev. Cancer.* 2002; 2: 563-72.

[29] **Kim J, Yu W, Kovalski K, Ossowski L.** Requirement for specific proteases in cancer cell intravasation as revealed by a novel semiquantitative PCR-based assay. *Cell.* 1998; 94: 353-62.

[30] **Adachi Y, Yamamoto H, Itoh F, Hinoda Y, Okada Y, Imai K.** Contribution of matrilysin (MMP-7) to the metastatic pathway of human colorectal cancers. *Gut.* 1999; 45: 252-8.

[31] **Montel V, Kleeman J, Agarwal D, Spinella D, Kawai K, Tarin D.** Altered metastatic behavior of human breast cancer cells after experimental manipulation of matrix metalloproteinase 8 gene expression. *Cancer Research.* 2004; 64: 1687-94.

[32] **Cao J, Chiarelli C, Kozarekar P, Adler HL.** Membrane type 1-matrix metalloproteinase promotes human prostate cancer invasion and metastasis. *Thromb. Haemost.* 2005; 93: 770-8.

[33] **Wyckoff JB, Jones JG, Condeelis JS, Segall JE.** A critical step in metastasis: in vivo analysis of intravasation at the primary tumor. *Cancer Res.* 2000; 60: 2504-11.

[34] **Koop S, Schmidt EE, MacDonald IC, Morris VL, Khokha R, Grattan M, Leone J, Chambers AF, Groom AC.** Independence of metastatic ability and extravasation: metastatic ras-transformed and control fibroblasts extravasate equally well. *Proc. Natl. Acad. Sci. U. S. A.* 1996; 93: 11080-4.

[35] **Xian X, Hakansson J, Stahlberg A, Lindblom P, Betsholtz C, Gerhardt H, Semb H.** Pericytes limit tumor cell metastasis. *J. Clin. Invest.* 2006; 116: 642-51.

[36] **Gerhardt H, Semb H.** Pericytes: gatekeepers in tumour cell metastasis? *J. Mol. Med.* 2008; 86: 135-44.

[37] **Taniguchi S, Takeoka M, Ehara T, Hashimoto S, Shibuki H, Yoshimura N, Shigematsu H, Takahashi K, Katsuki M.** Structural fragility of blood vessels and peritoneum in calponin h1-deficient mice, resulting in an increase in hematogenous metastasis and peritoneal dissemination of malignant tumor cells. *Cancer Res.* 2001; 61: 7627-34.

[38] **Plaisier M, Kapiteijn K, Koolwijk P, Fijten C, Hanemaaijer R, Grimbergen JM, Mulder-Stapel A, Quax PHA, Helmerhorst FM, van Hinsbergh VWM.** Involvement of membrane-type matrix metalloproteinases (MT-MMPs) in capillary tube formation by human endometrial microvascular endothelial cells: Role of MT3-MMP. *J. Clin. Endocrinol. Metab*. 2004; 89: 5828-36.

[39] **Plaisier M, Koolwijk P, Hanemaaijer R, Verwey RA, van der Weiden RM, Risse EK, Jungerius C, Helmerhorst FM, van Hinsbergh VW.** Membrane-type matrix metalloproteinases and vascularization in human endometrium during the menstrual cycle. *Mol. Hum. Reprod.* 2006; 12: 11-8.

[40] **Rizki A, Weaver VM, Lee SY, Rozenberg GI, Chin K, Myers CA, Bascom JL, Mott JD, Semeiks JR, Grate LR, Mian IS, Borowsky AD, Jensen RA, Idowu MO, Chen F, Chen DJ, Petersen OW, Gray JW, Bissell MJ.** A human breast cell model of preinvasive to invasive transition. *Cancer Res.* 2008; 68: 1378-87.

[41] **Wang Y, Johnson AR, Ye QZ, Dyer RD.** Catalytic activities and substrate specificity of the human membrane type 4 matrix metalloproteinase catalytic domain. *J. Biol. Chem.* 1999; 274: 33043-9.

[42] **Kolkenbrock H, Essers L, Ulbrich N, Will H.** Biochemical characterization of the catalytic domain of membrane-type 4 matrix metalloproteinase. *Biol. Chem.* 1999; 380: 1103-8.

[43] **Chantrain CF, Henriet P, Jodele S, Emonard H, Feron O, Courtoy PJ, DeClerck YA, Marbaix E.** Mechanisms of pericyte recruitment in tumour angiogenesis: a new role for metalloproteinases. *Eur. J. Cancer.* 2006; 42: 310-8.

[44] **Jodele S, Chantrain CF, Blavier L, Lutzko C, Crooks GM, Shimada H, Coussens LM, DeClerck YA.** The contribution of bone marrow-derived cells to the tumor vasculature in neuroblastoma is matrix metalloproteinase-9 dependent. *Cancer Res.* 2005; 65: 3200-8.

[45] **Lehti K, Allen E, Birkedal-Hansen H, Holmbeck K, Miyake Y, Chun TH, Weiss SJ.** An MT1-MMP-PDGF receptor-beta axis regulates mural cell investment of the microvasculature. *Genes Dev.* 2005; 19: 979-91.

[46] **Shofuda T, Shofuda K, Ferri N, Kenagy RD, Raines EW, Clowes AW.** Cleavage of focal adhesion kinase in vascular smooth muscle cells overexpressing membrane-type matrix metalloproteinases. *Arterioscler. Thromb. Vasc. Biol.* 2004; 24: 839-44.

[47] **Armulik A, Abramsson A, Betsholtz C.** Endothelial/pericyte interactions. *Circ. Res.* 2005; 97: 512-23.

[48] **Chen J, Somanath PR, Razorenova O, Chen WS, Hay N, Bornstein P, Byzova TV.** Akt1 regulates pathological angiogenesis, vascular maturation and permeability in vivo. *Nat. Med.* 2005; 11: 1188-96.

[49] **Hawighorst T, Velasco P, Streit M, Hong YK, Kyriakides TR, Brown LF, Bornstein P, Detmar M.** Thrombospondin-2 plays a protective role in multistep carcinogenesis: a novel host anti-tumor defense mechanism. *EMBO J.* 2001; 20: 2631-40.

[50] **Fears CY, Grammer JR, Stewart JE, Annis DS, Mosher DF, Bornstein P, Gladson CL.** Low-density lipoprotein receptor-related protein contributes to the antiangiogenic activity of thrombospondin-2 in a murine glioma model. *Cancer Res.* 2005; 65: 9338-46.

A Lymphatic network

LYVE-1 | QDOT

MT4-xenografted mice

T
S

A
T
I

CTR-xenografted mice

T
S

T
A
I

B Lymph node metastases

MT4-xenografted mice

A LN : 80 %

I LN : 60 %

Lung : 60 %

CTR-xenografted mice

A LN : 60 %

I LN : 70 %

Lung : 0 %

Method of lung metastasis detection

Models of lung metastasis

Spontaneous model (s.c. injection)

A — Luciferase in vivo: MT4 (Lung, 60%) | CTR (LN, 0%)

B — Ki-67 immunostaining: Nbr of metastatic foci / 45 fields vs MT4 clones, CTR clones. Severity 1, Severity 2, Severity 3. *** over MT4 Severity 1, * over MT4 Severity 2.
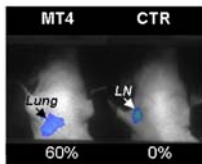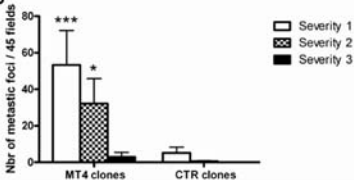
Experimental model (i.v. injection)

C — Luciferase in vivo: MT4 (100%) | CTR (80%)

D — Ki-67 immunostaining: Nbr of metastatic foci / 45 fields vs MT4 clones, CTR clones. Severity 1, Severity 2, Severity 3.
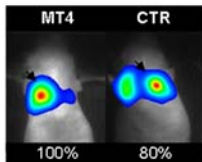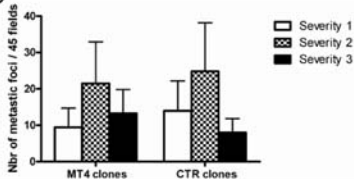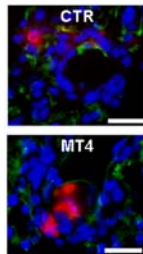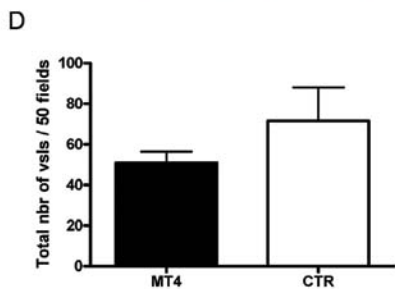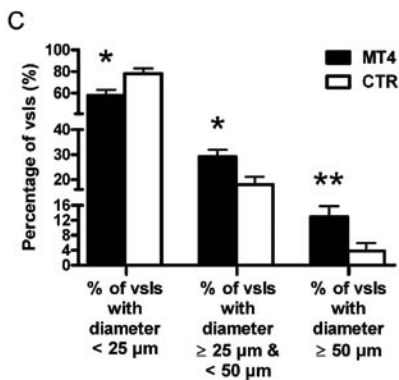
Short term extravasation (i.v. injection)

E — Cell tracker: CTR | MT4. Nbr of tumor cells / 20 fields vs MT4 clones, CTR clones.

Xenograft MT4 (panels A, C)

Xenograft CTR (panels B, D)

A **MT4** / B **CTR**

SMA
Lectin

C

Percentage of vsls (%)

■ MT4 □ CTR

* ** (grouped bar chart)

% of vsls with diameter < 25 µm

% of vsls with diameter ≥ 25 µm & < 50 µm

% of vsls with diameter ≥ 50 µm

D

Total nbr of vsls / 50 fields

MT4   CTR

E

Mean area / vsls (µm²)

MT4   CTR

F

Density of red staining

Distance from green staining (µm)

□ CTR
■ MT4

A

MT4   CTR

7 hrs

B

MT4   CTR

24 hrs

1280
998
715
433
150

C

MT4
CTR

**

7 hrs   24 hrs

Tumor / reference ratio